

# Triplet supercurrents in clean and disordered half-metallic ferromagnets

Matthias Eschrig<sup>1,\*</sup> and Tomas Löfwander<sup>1,†</sup>

<sup>1</sup>*Institut für Theoretische Festkörperphysik and DFG-Center for Functional Nanostructures, Universität Karlsruhe, D-76128 Karlsruhe, Germany*

\**e-mail: eschrig@tfp.uni-karlsruhe.de*

†*Present address: Department of Microtechnology and Nanoscience, Chalmers University of Technology, S-412 96 Göteborg, Sweden*

(Dated: December 4, 2006; Published in Nature Physics 4, 138-143 (2008).)

Interfaces between materials with differently ordered phases present unique opportunities to study fundamental problems in physics. One example is the interface between a singlet superconductor and a half-metallic ferromagnet, where Cooper pairing occurs between electrons with opposite spin on one side, while the other displays 100% spin polarisation. The recent surprising observation of a supercurrent through half-metallic CrO<sub>2</sub> therefore requires a mechanism for conversion between unpolarised and completely spin polarised supercurrents. Here we suggest a conversion mechanism based on electron spin precession together with triplet pair rotation at interfaces with broken spin-rotation symmetry. In the diffusive limit the triplet supercurrent is dominated by inter-related odd-frequency *s*-wave and even-frequency *p*-wave pairs. In the crossover to the ballistic limit additional symmetry components become relevant. The interface region exhibits a superconducting state of mixed-spin pairs with highly unusual symmetry properties that opens up new perspectives for exotic Josephson devices.

Half-metallic ferromagnets have great potential in the field of spintronics as sources of spin-polarised electric currents. Remarkably, they show conducting or insulating behaviour depending on the direction of the electron spin. Since only a few such half metals are known, among them La<sub>2/3</sub>Ca<sub>1/3</sub>MnO<sub>3</sub> [1] and CrO<sub>2</sub> [2], their characterisation has attracted great attention. Half metals, when contacted with other materials such as superconductors, can also be used as well controlled test-laboratories to study the interplay between different types of orders.

Recently, Keizer *et.al* [2] reported a Josephson supercurrent between two singlet superconducting electrodes (NbTiN) separated by a wide region of CrO<sub>2</sub>. In a half metal only conduction electrons with equal spin can be paired, since the other spin species is insulating. Currently, the mechanism involved in the conversion process between singlet Cooper pairs ( $(|\uparrow\downarrow\rangle - |\downarrow\uparrow\rangle)/\sqrt{2}$ ) and equal-spin pairs  $|\uparrow\uparrow\rangle$  at the interfaces between the materials remains highly controversial. Moreover, the symmetries of the relevant pairing correlations mediating the triplet supercurrent and their dependence on the amount of disorder is currently debated. It is claimed [3, 4] that the main source of the triplet Josephson current in diffusive ferromagnets is odd-frequency *s*-wave pairing amplitudes. On the other hand, it has been shown that in clean half metals also *p*-wave triplet pairing amplitudes are important [5].

Consider the Josephson junction in Fig. 1. It consists of a half metal extending from  $x_1$  to  $x_2$ , sandwiched between two singlet superconductors. When a phase difference  $\chi_2 - \chi_1$  exists between the superconducting order parameters, an exotic form of Josephson effect occurs: a singlet supercurrent,  $j_{singlet}$  (blue in Fig. 1), is converted to an equal-spin triplet supercurrent,  $j_{triplet}$  (yellow in

Fig. 1), within an interface layer extending about a superconducting coherence length into the electrodes. The equal-spin triplet supercurrent flows through the half-metallic material, while the singlet part is completely blocked. The sum of the singlet and triplet currents is constant, obeying the continuity equation.

The mechanism of the current conversion we propose in this paper leads to a natural explanation of several findings of the experiment [2]: (i) a finite Josephson current in the half metal; (ii) hysteretic shifts of the equilibrium

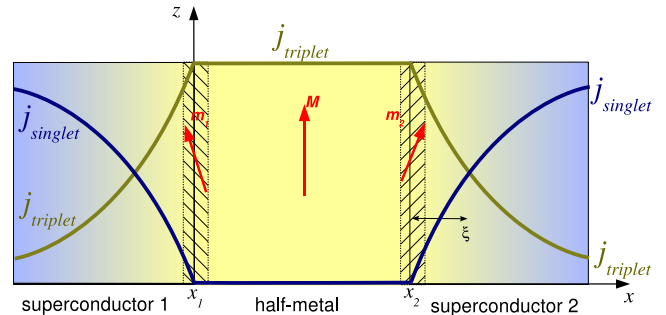


**FIG. 1: Conversion between singlet and triplet supercurrents.** We consider two singlet superconductor banks separated by a half-metallic ferromagnetic layer with magnetisation vector  $\mathbf{M}$ . Spin-rotation symmetry around  $\mathbf{M}$  is broken at the interfaces (shaded), characterised by misaligned averaged interface moments  $\mathbf{m}_1$  and  $\mathbf{m}_2$ . As a consequence, inside the superconductors within a coherence length from the interfaces, there is a conversion from a supercurrent of singlet Cooper pairs ( $j_{singlet}$ , blue line) to a supercurrent of triplet Cooper pairs ( $j_{triplet}$ , green line), as illustrated by the shading from blue to yellow. Only the triplet supercurrent can penetrate the half metal.

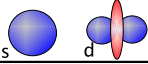
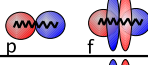
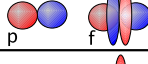

Spin	Frequency	Momentum
Singlet (odd)	Even	Even 
	Odd	Odd 
Triplet (even)	Even	Odd 
	Odd	Even 

TABLE I: **The four classes of superconducting correlations following from the Pauli principle.** All four symmetry components are induced in the superconducting regions next to the interface, but only the  $\uparrow\uparrow$ -triplet ones in the half metallic region. The dominating orbital contributions to the supercurrents in the half metal are shown in the lower two lines (triplet): even frequency  $p$ -wave and  $f$ -wave, and odd frequency  $s$ -wave and  $d$ -wave. Wavy lines symbolise the dynamical nature of the odd frequency amplitudes.

phase difference over the junction depending on the magnetic pre-history; (iii) Josephson junctions involving half metals are  $\pi$ -junctions after subtraction of the hysteretic shifts; (iv) sample-to-sample fluctuations in the magnitude of the critical current.

The four symmetry types of Cooper pairs allowed by the Pauli exclusion principle [6, 7] are listed in Table I. We show that in moderately disordered half metals the supercurrent is carried predominantly by odd-frequency  $s$ -wave and  $d$ -wave amplitudes, multiplied with even frequency  $p$ -wave and  $f$ -wave amplitudes. In the diffusive limit the supercurrent is dominated by the product of the  $s$ -wave and the  $p$ -wave amplitudes. We find that a peak in the temperature dependence of the critical current, previously predicted for clean half metals [5], is a robust feature also for disordered half metals. We study the entire crossover from the ballistic to the diffusive regime.

## SPIN-MIXING AND TRIPLET-ROTATION

The conversion process between the singlet and equal-spin triplet supercurrents is triggered by two important phenomena taking place at the interface: (i) spin mixing provides  $S = 1$ ,  $m = 0$  triplet correlations near the interface, and (ii) breaking of spin-rotation symmetry with respect to the magnetisation axis  $\mathbf{M}$  in the half metal allows for this  $m = 0$  triplet to be rotated into an  $S = 1$ ,  $m = 1$  triplet amplitude. Note that both phenomena are required for a non-vanishing Josephson effect.

Spin-mixing is the result of different scattering phase shifts that electrons with opposite spin acquire when scattered (reflected or transmitted) from an interface [8–10]. It results from either a spin-polarisation of the interface potential, or differences in the wave-vector mis-

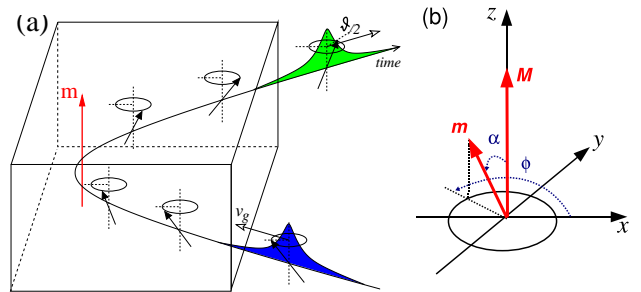


FIG. 2: **Spin mixing and broken spin-rotation symmetry around  $\mathbf{M}$ .** (a) The spin-mixing angle  $\vartheta$  corresponds to the precession of a spin around the magnetisation  $\mathbf{m}$  when a wave packet penetrates into the classically forbidden interface region. The spin component along  $\mathbf{m}$  acquires a spin-dependent scattering phase. (b) Definition of the polar angles  $\alpha$  and  $\varphi$  for an interface moment  $\mathbf{m}$  misaligned with respect to  $\mathbf{M}$ .

matches for spin up and spin down particles at either side of the interface, or both. It is a robust and ubiquitous feature for interfaces involving strongly spin-polarised ferromagnets. Another, equivalent, way of discussing spin-mixing, shown in Fig. 2(a), is in terms of a spin-precession around  $\mathbf{M}$  when wave packets penetrate the interface region.

Broken spin-rotation symmetry leads to spin-flip processes at the interfaces. Its origin is more subtle and deserves special attention. We discuss in the Supplementary Information some possible origins of misalignment of the interface moments with respect to the bulk magnetic moment relevant for the material  $\text{CrO}_2$ . Magnetic materials often display surface order that is different from the bulk order, possibly with disordered surface phases. Here we only assume that the *averaged* interface magnetic moment deviates from the direction of the bulk magnetisation. A possible insulating magnetic interface layer is also described by our theory. The exact microscopic distribution of local moments at the interface is not important for superconducting phenomena, since Cooper pairs are of the size of the coherence length  $\xi$  which is much larger than the atomic scale. It is, however, important for the effective interface scattering matrix, as it can lead to spin-flip terms if the distribution of the local-moment directions breaks spin-rotation symmetry around  $\mathbf{M}$ .

The two above-mentioned effects, spin-mixing and broken spin-rotation symmetry around  $\mathbf{M}$ , are interface properties and lead to the appearance of the long-range  $m = 1$  triplet correlations in the half metal as seen schematically in Fig. 3. This is in contrast to the case of a weak ferromagnet coupled to a superconductor, where without either large scale inhomogeneities (e.g. domain wall structures near the interfaces) or strongly enhanced interface magnetism such correlations are negligible.

To quantify the above discussion, we employ a simple model that is formulated in terms of an interface

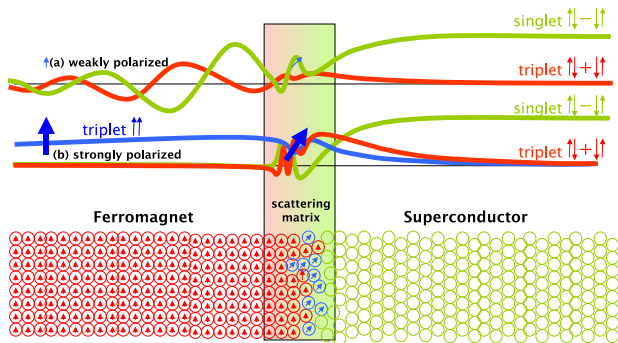


FIG. 3: **Proximity amplitudes induced at superconductor-ferromagnet interfaces.** (a) Misaligned spins in the interface region (described by a scattering matrix) add little to the main effect for weakly polarised ferromagnets, an out-of-phase oscillation of a singlet and a  $\uparrow\downarrow + \downarrow\uparrow$  ( $m = 0$ ) triplet component in the ferromagnet. (b) For strongly polarised ferromagnets a considerable  $m = 0$  triplet amplitude is induced in the superconductor by the strong interface spin polarisation. Disordered interface moments rotate this  $m = 0$  into a  $\uparrow\uparrow$  ( $m = 1$ ) triplet amplitude in the ferromagnet, if the averaged interface moment is misaligned with the bulk magnetisation.

scattering matrix, which connects incoming to outgoing waves in the asymptotic regions [5]. The scattering matrix depends in general on the following parameters: (i) the total transmission  $t$  between the superconductor and the half metal; (ii) the orientation of the averaged interface magnetic moment,  $\mathbf{m}$ , with polar angles  $\alpha$  and  $\varphi$  as shown in Fig. 2(b); (iii) two spin-mixing angles, one for reflection ( $\vartheta$ ) and one for transmission ( $\vartheta_{\uparrow\uparrow}$ ). The most general form of the scattering matrix for the tunnelling limit, apart from irrelevant spin-independent phases, has the form (see the Supplementary Information)

$$\hat{\mathbf{S}} = \left( \begin{array}{cc|c} e^{\frac{i}{2}\vartheta} & 0 & t_{\uparrow\uparrow}e^{i(\vartheta_{\uparrow\uparrow} + \frac{\vartheta}{4})} \\ 0 & e^{-\frac{i}{2}\vartheta} & t_{\downarrow\uparrow}e^{i(\vartheta_{\downarrow\uparrow} - \frac{\vartheta}{4})} \\ \hline t_{\uparrow\uparrow}e^{-i(\vartheta_{\uparrow\uparrow} - \frac{\vartheta}{4})} & t_{\downarrow\uparrow}e^{-i(\vartheta_{\downarrow\uparrow} + \frac{\vartheta}{4})} & -1 \end{array} \right). \quad (1)$$

Here,  $t_{\uparrow\uparrow} = t \cos \frac{\alpha}{2}$  and  $t_{\downarrow\uparrow} = t \sin \frac{\alpha}{2}$  are transmission amplitudes from the two superconducting spin bands to the conducting half-metallic spin- $\uparrow$  band, and  $\vartheta$ ,  $\vartheta_{\uparrow\uparrow}$ , and  $\vartheta_{\downarrow\uparrow} = \pi + \varphi + \vartheta_{\uparrow\uparrow}$  are spin-mixing angles. Each interface  $j = 1, 2$  is characterised by the five parameters  $t_j$ ,  $\alpha_j$ ,  $\varphi_j$ ,  $\vartheta_j$ , and  $\vartheta_{\uparrow\uparrow j}$ , that in general can depend on the direction of incoming quasiparticles. An alternative set is  $t_{\uparrow j}$ ,  $t_{\downarrow j}$ ,  $\vartheta_{\uparrow j}$ ,  $\vartheta_{\downarrow j}$ , and  $\vartheta_{\downarrow\uparrow j}$ . The presence of the spin-flip term  $t_{\downarrow\uparrow}e^{i\vartheta_{\downarrow\uparrow}}$  in the scattering matrix, equation (1), is a direct consequence of the broken spin-rotation symmetry around  $\mathbf{M}$  at the interface.

## INDIRECT JOSEPHSON EFFECT

In the following we calculate the Josephson current through the junction to leading order in  $t$  and  $\vartheta$ . This approximation is not essential, but simplifies the following discussion while all important phenomena are captured. The presence of an  $m = 0$  triplet amplitude with a magnitude proportional to  $\sin \vartheta$  [see equation (2) below] is accompanied by a suppression of the singlet pairing amplitudes proportional to  $\sin^2 \frac{\vartheta}{2}$  in the superconductors near the interface (see Supplementary Table S1), as illustrated in Fig. 3 (green lines) [5, 7, 8]. It leads to corrections to the singlet order parameter  $\Delta$  that are second order in  $\vartheta$ . Thus, to leading order, the corresponding suppression of  $\Delta$  can be neglected. It follows that Anderson's theorem [11, 12] holds and  $\Delta$  is also insensitive to impurity scattering (note, however, that in the *immediate* interface region described by the scattering matrix the gap is dramatically suppressed, e.g. due to diffusion of magnetic moments; this effect is included in our theory). For simplicity we consider the case of equal gap magnitudes in the two superconductors,  $\Delta_j = |\Delta|e^{i\chi_j}$ , for superconductors  $j = 1$  and  $j = 2$ , see Fig. 1.

Due to spin mixing at the interfaces a spin triplet ( $S = 1$ ,  $m = 0$ ) amplitude  $f_{t_{0j}}(x)$  is developed that extends from the interfaces about a coherence length into each superconductor,

$$f_{t_{0j}}(x) = i\pi|\Delta|e^{i\chi_j} \sin \vartheta_j \frac{|\varepsilon_n| \Psi_{0j}^s(x) + \Omega_n \Psi_{0j}^a(x)}{\Omega_n^2}, \quad (2)$$

where  $\Omega_n = \sqrt{\varepsilon_n^2 + |\Delta|^2}$ . We have separated the influence of the interfaces from that of the disorder in the bulk materials by introducing the real functions  $\Psi_{0j}^{s,a}(x)$ . The superscript denotes symmetric ( $s$ ) and antisymmetric ( $a$ ) components with respect to  $\mu = \cos(\theta_p)$ , where  $\theta_p$  is the angle between the Fermi velocity and the  $x$ -axis. In the clean limit,  $\Psi_{0j}^a(x) = -\frac{\text{sgn}(\mu)}{2}e^{-|x-x_j|/\xi_S|\mu|}$  and  $\Psi_{0j}^s(x) = \frac{\text{sgn}(\varepsilon_n)}{2}e^{-|x-x_j|/\xi_S|\mu|}$  where  $\xi_S = v_S/2\Omega_n$ , and  $v_S$  is the Fermi velocity in the superconductor. For an arbitrary impurity concentration the  $\Psi$ -functions are modified and must be calculated numerically for each given value of mean free path (see Supplementary Fig. S1).

The induced  $m = 0$  triplet amplitude derived above, together with the presence of spin-flip tunnelling amplitudes, leads to an equal-spin ( $m = 1$ ) pairing amplitude  $f_{\uparrow\uparrow}(x)$  in the half metal. The singlet component in the superconductor, being invariant under rotations around any quantisation axis, is not directly involved in the creation of the triplet in the half metal. A picture of an indirect Josephson effect emerges, therefore, that is mediated by the appearance of the  $m = 0$  triplet amplitudes in the superconductor.

In the tunnelling limit it is convenient to split the pairing amplitude in the half metal into contributions induced at the left and right interfaces:  $f_{\uparrow\uparrow} = f_{\uparrow\uparrow 1} + f_{\uparrow\uparrow 2}$ ,

with momentum-symmetric and antisymmetric components

$$f_{\uparrow\uparrow j}^{s,a}(x) = 2\pi i A_j |\Delta| e^{i\bar{\chi}_j} \frac{|\varepsilon_n|}{\Omega_n^2} \Psi_j^{s,a}(x), \quad (3)$$

where the amplitude is given by

$$A_j = 2t_{\uparrow\uparrow j} t_{\downarrow\uparrow j} \sin\left(\frac{\vartheta_j}{2}\right) = t_j^2 \sin(\alpha_j) \sin\left(\frac{\vartheta_j}{2}\right), \quad (4)$$

and the effective phase by

$$\bar{\chi}_j = \chi_j + (\vartheta_{\uparrow\uparrow j} - \vartheta_{\downarrow\uparrow j}) = \chi_j - (\pi + \varphi_j). \quad (5)$$

In equation (3), we have separated the contributions from the interface scattering and the contributions from the disorder in the half metal by introducing the (real) functions  $\Psi_j^{s,a}$ .

The Josephson current reads [see also equation (S13) in the Supplementary Information]

$$J_x = -J_c \sin(\bar{\chi}_2 - \bar{\chi}_1), \quad (6)$$

where the critical current density is given by

$$J_c = J_0 \frac{T}{T_c} \sum_{\varepsilon_n > 0} \frac{|\Delta|^2 \varepsilon_n^2}{\Omega_n^4} \langle \mu A_1 A_2 (\Psi_2^s \Psi_1^a - \Psi_1^s \Psi_2^a) \rangle. \quad (7)$$

Here, the current unit is  $J_0 = 4\pi e v_H N_H T_c$ ,  $N_H$  is the density of states at the Fermi level in the half metal,  $e$  is the electron charge, and  $\langle \dots \rangle = \int_0^1 d\mu \dots$ .

Equations (4)-(7) describe an exotic Josephson effect in several respects. Equation (5) is related to the phase dependence of the Josephson effect and can be tested for example by studying the magnetic field dependence of the critical current. For a half metal, there can be extra phases that lead to shifts of the usual Fraunhofer pattern [7, 13]. Within our model there are contributions  $\delta\varphi = \varphi_2 - \varphi_1$  to the phases that depend on the microscopic structure of the disordered magnetic moments at the two interfaces. In particular, if the averaged magnetic interface moments  $\mathbf{m}_1$  and  $\mathbf{m}_2$  are non-collinear in the plane perpendicular to  $\mathbf{M}$ , such phases arise. The microstructure can be affected for example by applying a magnetic field that leads to hysteretic shifts  $\delta\varphi(H)$  of the equilibrium positions depending on the magnetic pre-history. When subtracting the shifts, the junction shows the typical characteristics of a  $\pi$ -junction [14], as revealed by the minus-sign in equation (6). The possibility to manipulate the shifts  $\delta\varphi$  with an external field yields a way to measure the relative orientation of  $\mathbf{m}_1$  and  $\mathbf{m}_2$  at the two interfaces. Finally, the critical Josephson current is proportional to the sine of the spin-mixing angles  $\vartheta_j/2$ , the transmission probabilities  $t_j^2$ , and the sine of the angles  $\alpha_j$  between  $\mathbf{m}_j$  and  $\mathbf{M}$ . This points to a strong sensitivity of the critical Josephson current to interface properties and is expected to lead to strong sample-to-sample variations. Note that none of the above parameters need to be small, such that critical currents of the order of that for normal junctions are possible. All these findings are in agreement with the experiment [2].

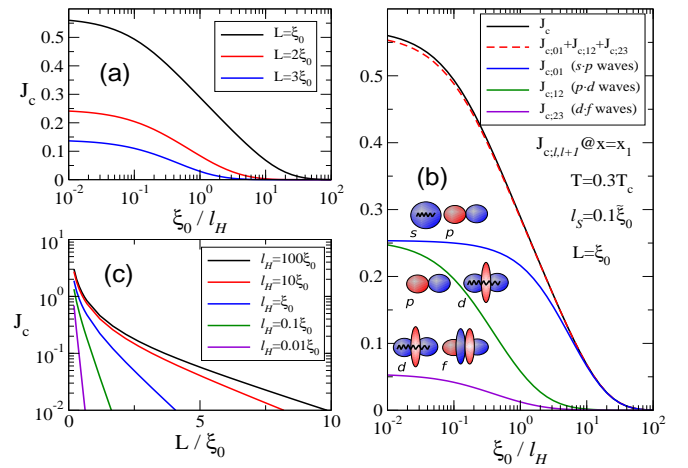


FIG. 4: **Critical Josephson current  $J_c$ .** (a) In the crossover from the ballistic to the diffusive limits  $J_c$  is monotonously suppressed. (b) In the crossover region, contributions to  $J_c$  from higher partial waves ( $l \geq 2$ ,  $d$ -wave,  $f$ -wave, etc.) are suppressed. In the diffusive limit the current (black line) is given by a product of  $s$ -wave ( $l = 0$ ) and  $p$ -wave ( $l = 1$ ) components (blue line). (c) For given mean free path  $\ell_H$ ,  $J_c$  is exponentially suppressed with junction length  $L$ . The unit for  $J_c$  is  $J_0 A_1 A_2 / 4\pi$ . The length unit is  $\xi_0 = v_H / 2\pi T_c$ . We assumed an anisotropy of  $t$  proportional to  $|\mu|$ .

## ROLE OF DISORDER

We now proceed with a detailed description of the role of disorder in the materials. For definiteness, in the remaining discussion we keep the mean free path in the superconducting banks fixed to  $\ell_S = 0.1\xi_0$  with  $\xi_0 = v_S / 2\pi T_c$ , and vary the mean free path of the half metal. It is well known that anisotropic superconducting correlations are sensitive to impurity scattering. Studies of unconventional superconductivity reveal that superconductivity disappears at a critical impurity concentration [9, 15]. This is however not the case for the proximity induced pairing amplitudes studied here. In Fig. 4 we show results for the critical Josephson current as function of the elastic mean free path, normalised to  $\xi_0 = v_H / 2\pi T_c$ . As shown in Fig. 4(a), the critical current is monotonously suppressed for decreasing mean free path, from the ballistic (left part of the abscissa in the figure) to the diffusive (right part) limits. The suppression is exponential in the diffusive limit, with a crossover taking place at a mean free path  $\ell_H$  comparable with the clean limit coherence length  $\xi_c = v_H / 2\pi T$ .

The critical Josephson current can be rewritten as a sum of terms, each consisting of products of neighbouring momentum symmetry components of the functions  $\bar{\Psi}_j \equiv A_j \Psi_j$  in equation (7), i.e.  $J_c = \sum_{l=0}^{\infty} J_{c;l,l+1}$ , where  $l = 0, 1, 2, 3, \dots$  denotes the  $s$ -,  $p$ -,  $d$ -,  $f$ -wave etc. pairing components (see the Supplementary Information). We have verified (see Supplementary Fig. S2) that for ballistic systems the  $p$ -wave amplitudes are larger than

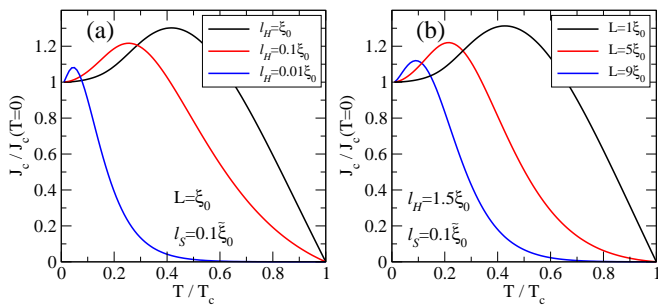


FIG. 5: **Non-monotonic temperature dependence.** (a) The critical Josephson current  $J_c$  has a maximum at a low temperature that for a specific junction length (here  $L = \xi_0 = v_H/2\pi T_c$ ) depends on the mean free path  $\ell_H$  in the half metal.  $J_c$  has been normalised to the zero-temperature value. In (b) we show the normalised current as function of junction length  $L$  for a fixed  $\ell_H = 1.5\xi_0$ . When the junction becomes effectively long compared with the diffusive limit coherence length,  $L = \xi_0 \gg \xi_d(T)$ , the current is dramatically suppressed [see Fig. 4(a)] and the peak is shifted to a lower temperature.

the  $s$ -wave amplitudes near the interfaces, while the opposite holds for diffusive systems. The amplitudes are tied to each other through the following general relation between the momentum-antisymmetric and the momentum symmetric parts:  $f_{\uparrow\uparrow}^a = -\text{sgn}(\varepsilon_n)\mu\xi_H\partial_x f_{\uparrow\uparrow}^s$ , where  $\xi_H^{-1} = \ell_H^{-1} + 2|\varepsilon_n|/v_H$ . In the diffusive limit, there is an additional relation,  $f_{\uparrow\uparrow}^{p\text{-wave}} = -\text{sgn}(\varepsilon_n)\ell_H\partial_x f_{\uparrow\uparrow}^{s\text{-wave}}$ . It follows that the *magnitudes* of the amplitudes differ (their ratio depends on the amount of disorder) while the *decay lengths* of the two are always identical, crossing over from the ballistic coherence length  $\xi_c = v_H/2\pi T$  to the diffusive coherence length  $\xi_d = \sqrt{\ell_H\xi_c/3}$ .

The first three terms of the partial wave expansion of the critical current are shown in Fig. 4(b). The sum of these contributions (red dashed line), composed of the  $s \cdot p$  (blue),  $p \cdot d$  (green), and  $d \cdot f$  (purple) components, amounts already to almost the entire current (black line). In the diffusive limit, the current is carried almost exclusively by the product of the even-frequency  $p$ -wave and the odd-frequency  $s$ -wave pairing amplitudes (blue). In the crossover region to ballistic transport there is an onset of contributions from higher order partial waves  $l \geq 2$ . It is clear from the figure, that for  $\ell_H \geq \xi_0$  the diffusive Usadel approximation breaks down. Note that in the half metal only partial waves compatible with the spin triplet combinations of Table I are possible, as indicated in Fig. 4(b).

In Fig. 4(c) we show for several mean free paths the dependence of the critical current on the junction length  $L$ . A rapid exponential suppression of the effect with junction length is observed in the diffusive limit, whereas in the moderately disordered region a considerable effect is expected for junction lengths up to 5-10 coherence lengths.

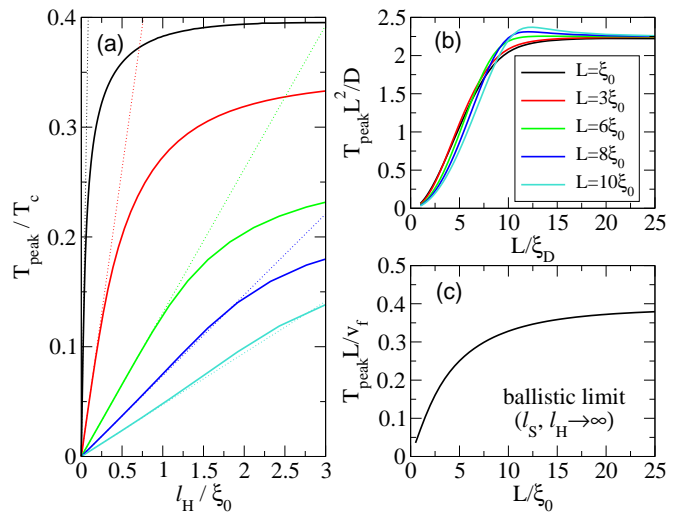


FIG. 6: **Peak position  $T_{peak}$  in  $J_c(T)$ .** (a)  $T_{peak}$  as function of the mean free path  $\ell_H$  in the half metal (full lines).  $T_{peak}$  approaches linearly zero temperature with decreasing  $\ell_H$ . The corresponding slope characterises  $T_{peak}$  in the diffusive limit, and is well described by the formula  $T_{peak} = 2.25E_{Th}$  (shown as dotted lines), with the Thouless energy  $E_{Th} = D/L^2$  and the diffusion constant  $D = v_H\ell_H/3$ . (b) Scaling plot with  $T_{peak}/E_{Th}$  as a function of  $L/\xi_D$  with  $\xi_D = \sqrt{D/2\pi T_c}$ . (c)  $T_{peak}$  for the clean limit normalised to  $v_H/L$  as a function of  $L/\xi_0$ , showing for long junctions a scaling of  $T_{peak}$  with  $v_H/L$ .

In Fig. 5 we discuss the influence of disorder on the temperature dependence of the critical current. We have normalised all  $J_c(T)$  curves to their zero-temperature value. There is a characteristic peak appearing at a temperature below  $\sim T_c/2$  as predicted for ballistic systems in Ref. [5]. The origin of the peak is the factor  $|\Delta|^2\varepsilon_n^2/\Omega_n^4$  in equation (7), that results from the odd-frequency pairing amplitudes on the *superconducting sides* of the interfaces being the sources of the equal-spin correlations in the half metal, as revealed by the factor  $|\Delta||\varepsilon_n|/\Omega_n^2$  in equation (3). These amplitudes have a dynamical degree of freedom, that makes them less effective compared to even frequency amplitudes when the lowest Matsubara energy  $\pi T$  drops below  $\Delta(T)$ . Whereas this gives  $T_{peak} \sim \Delta(T_{peak})/\pi$  for ballistic short ( $L \leq \xi_0$ ) junctions, in the case of long or disordered junctions  $T_{peak}$  is determined by the smaller Thouless energy. This shift to lower temperatures with decreasing  $\ell_H$  is seen in Fig. 5(a). Conversely, for a particular mean free path, the peak is shifted to lower temperatures for increasing  $L$ , as shown in Fig. 5(b) for  $\ell_H = 1.5\xi_0$ . For long junctions the critical current has a characteristic exponential temperature dependence above the peak.

In Fig. 6(a) we show the peak temperature,  $T_{peak}$ , for a number of junction lengths and a wide range of mean free paths. For large mean free paths the peak position levels off ( $T_{peak}$  is independent of the mean free path for clean systems), while for small mean free paths, there is

a linear relation  $T_{peak} \propto \ell_H$ , implying that  $T_{peak}$  vanishes in the limit  $\ell_H \rightarrow 0$ . However, the diffusive limit is defined as  $\ell_H \rightarrow 0$  and  $\xi_0 \rightarrow \infty$  keeping  $\xi_D = \sqrt{\ell_H \xi_0 / 3}$  finite. In Fig. 6 (b) we show the same data as in (a), but plotted as function of the only dimensionless diffusive length scale parameter  $L/\xi_D$ , and the position of the peak in units of the Thouless energy  $E_{Th} = D/L^2$  (diffusion constant  $D = v_H \ell_H / 3$ ). The diffusive limit here corresponds to the curves for which  $\ell_H / \xi_0 \ll 1$ , i.e.  $L/\xi_D \gg L/\xi_0$ . In the limit of small diffusion length,  $\xi_D \rightarrow 0$ , all curves approach the value  $T_{peak} \approx 2.25 E_{Th}$ . This is the region where the diffusive (thermal) coherence length  $\xi_d = \xi_D \sqrt{T_c/T}$  is smaller than  $L$ . The spread of the curves in Fig. 6(b) is due to deviations from diffusive behaviour, which leads to additional dependences on the ballistic parameter  $L/\xi_0$ . For long junctions in the clean limit ( $L \gg \xi_c$ ), the ballistic Thouless energy  $v_H/L$  is the relevant energy scale for  $T_{peak}$ , as seen in Fig. 6(c).

## IMPLICATIONS FOR EXPERIMENT

Since the peak survives the crossover from the ballistic to the diffusive limit, it serves as a true fingerprint of equal-spin triplet correlations in the half metal. For moderately disordered junctions, the peak is readily measurable experimentally when  $L$  is of the order of the coherence length at  $T_c$ . The peak is best observed in the limit of large Thouless energy, because then the dominating energy scale is set by the energy of the odd-frequency pairing amplitudes. Note, finally, that in contrast to Josephson junctions that involve weak ferromagnets, no oscillating amplitudes are involved in half metals, thus ruling out precursor effects of a 0 to  $\pi$  transition.

Turning to Ref. [2], the low-temperature resistivity of the  $\text{CrO}_2$  material of  $8.9 \mu\Omega \text{ cm}$  implies a mean free path of  $\ell_H \approx 40 \text{ nm}$  (note that the film thickness of  $100 \text{ nm}$  was considerably larger than that). From band structure calculations, the Fermi velocity for  $\text{CrO}_2$  is  $v_H \approx 2.2 \times 10^5 \text{ m/s}$  [16], implying  $\xi_0 \approx 27 \text{ nm}$ , or  $\xi_0/\ell_H \approx 2/3$  (for  $T = 0.3T_c$  this gives  $\xi_c \approx 90 \text{ nm}$  and  $\xi_d \approx 35 \text{ nm}$ ). The  $\text{CrO}_2$  of Ref. [2] is therefore moderately disordered, being in the crossover region in Fig. 4(b), rather than in the clean or diffusive limits. With the typical length of  $\text{CrO}_2$  in [2] of  $L \approx 300 \text{ nm} \approx 11\xi_0$ , we can from Figs. 5(b) and 6(a) predict that if measurements are extended to lower temperatures, or a shorter junction length is used, a peak in  $J_c(T)$  should be observed.

- [3] Volkov, A. F., Bergeret, F. S. & Efetov, K. B. Odd Triplet Superconductivity in Superconductor-Ferromagnet Multilayered Structures. *Phys. Rev. Lett.* **90**, 117006 (2003).
- [4] Asano, Y., Tanaka, Y. & Golubov, A. A. Josephson Effect due to Odd-frequency Pairs in Diffusive Half Metals. *Phys. Rev. Lett.* **98**, 107002 (2007).
- [5] Eschrig, M., Kopu, J., Cuevas, J. C. & Schön, G. Theory of Half-Metal/Superconductor Heterostructures. *Phys. Rev. Lett.* **90**, 137003 (2003).
- [6] Tanaka, Y., & Golubov, A. A. Theory of the Proximity Effect in Junctions with Unconventional Superconductors. *Phys. Rev. Lett.* **98**, 037003 (2007).
- [7] Eschrig, M. *et al.* Symmetries of Pairing Correlations in Superconductor-Ferromagnet Nanostructures. *J. Low Temp. Phys.* **147**, 457-476 (2007).
- [8] Tokuyasu, T., Sauls, J. A. & Rainer, D. Proximity effect of a ferromagnetic insulator in contact with a superconductor. *Phys. Rev. B* **38**, 8823-8833 (1988).
- [9] Sigrist, M., & Ueda, K. Phenomenological theory of unconventional superconductivity. *Rev. Mod. Phys.* **63**, 239-311 (1991).
- [10] Kopu, J., Eschrig, M., Cuevas, J. C. & Fogelström, M. Transfer-matrix description of heterostructures involving superconductors and ferromagnets. *Phys. Rev. B* **69**, 094501 (2004).
- [11] Anderson, P. W. Theory of dirty superconductors. *J. Phys. Chem. Solids* **11**, 26-30 (1959).
- [12] Abrikosov, A. A. & Gor'kov, L. P. Superconducting alloys at finite temperatures. *Zh. Eksp. Teor. Fiz.* **36**, 319-320 (1959) [*Sov. Phys. JETP* **9**, 220-221 (1959)].
- [13] Braude, V. & Nazarov, Yu. V. Fully developed triplet proximity effect. *Phys. Rev. Lett.* **98**, 077003 (2007).
- [14] Buzdin, A. I., Bulaevskii, L. N. & Panyukov, S. V. Critical-current oscillations as a function of the exchange field and thickness of the ferromagnetic metal (F) in an S-F-S Josephson junction. *Pis'ma Zh. Eksp. Teor. Fiz.* **35**, 147-148 (1982) [*Sov. Phys. JETP Lett.* **35**, 178-180 (1982)].
- [15] Larkin, A. I. Vector pairing in superconductors of small dimensions. *Pis'ma Zh. Eksp. Teor. Fiz.* **2**, 205-209 (1965) [*Sov. Phys. JETP Lett.* **2**, 130-133 (1965)].
- [16] Lewis, S. P., Allen, P. B. & Sasaki, T. Band structure and transport properties of  $\text{CrO}_2$ . *Phys. Rev. B* **55**, 10253-10260 (1997).

**Author information:** Correspondence and requests for materials should be directed to M.E. (eschrig@tfp.uni-karlsruhe.de).

**Acknowledgments:** The authors would like to thank Juha Kopu and Gerd Schön for important contributions, Anna Posazhennikova for comments on the manuscript, Ulrich Rüdiger for discussions on interface properties of ferromagnets, and Ruurd Keizer and Teun Klapwijk for communications in relation to Ref. [2]. T.L. acknowledges financial support from the Alexander von Humboldt Foundation. M.E. acknowledges hospitality of the Aspen Center for Physics.

**Author contributions:** M.E. and T.L. shared equal responsibility for all aspects of this project.

**Competing financial interests:** The authors declare no competing financial interests.

**Supplementary Information** accompanies this paper on [www.nature.com/naturephysics](http://www.nature.com/naturephysics).

- [1] Chakhalian, J. *et al.* Magnetism at the interface between ferromagnetic and superconducting oxides. *Nature Physics* **2**, 244-248 (2006).
- [2] Keizer, R.S. *et al.* A spin triplet supercurrent through the half-metallic ferromagnet  $\text{CrO}_2$ . *Nature* **439**, 825-827 (2006).

## SUPPLEMENTARY MATERIAL

### Characterisation of interfaces with CrO<sub>2</sub>

Although our theory is general and by no means restricted to a specific material, it is useful to discuss several possible reasons for the existence of misaligned moments in the interface region relevant for experiment [1]. It has been shown recently [2] that the CrO<sub>2</sub> films used in experiment [1] have a homogeneous magnetisation profile throughout the film, but with a magnetisation direction that is non-collinear with the magnetisation direction of bulk CrO<sub>2</sub>, as a result of the epitaxial coherence strain at the interface between the substrate and CrO<sub>2</sub>. There are two possible ground states, and consequently the CrO<sub>2</sub> film shows a biaxial asymmetry. Using such biaxial CrO<sub>2</sub> films, Keizer *et al.* reported the above mentioned long-range Josephson effect [1]. The magneto-crystalline anisotropy due to spin orbit coupling is uniaxial.

The interface between CrO<sub>2</sub> and NbTiN should be considered rather rough, in particular for the preparation technique used in [1]. In experiment [1], a well known antiferromagnetic Cr<sub>2</sub>O<sub>3</sub> layer at the CrO<sub>2</sub>-surface has been removed before contacting with the superconductor NbTiN. Here, several possible sources for moment misalignment at the interface between the half metallic ferromagnet CrO<sub>2</sub> and the superconductor NbTiN need to be considered. (A) Interface magnetic anisotropy can dominate the bulk anisotropy leading to interface magnetism with a moment perpendicular to the bulk magnetisation. However, in CrO<sub>2</sub> the shape anisotropy is very strong and such interface magnetism is only plausible if disorder or roughness of the interface weakens the exchange coupling between the interface spins and the bulk spins. (B) An interface with finite roughness will have a reduced exchange coupling of interface spins to bulk spins in certain regions. As the direction of the bulk spins is determined non-locally by an interplay between the strain of the substrate and the uniaxial anisotropy, it will in general deviate from the direction of the spins that do not feel such an influence of the substrate. As a result misalignment of a considerable number of interface spins is probable. (C) If clusters of spins are formed in the interface region, it has been shown [3] that the magnetic coupling between the Cr sites oscillates from antiferromagnetic to ferromagnetic and back when successively adding an oxygen atom. Thus, the interplay between shape anisotropy of the clusters, the crystalline anisotropy within a cluster, and the magnetic coupling between the clusters and the bulk magnetisation will ultimately determine the effective magnetisation of the interface. Given the fact, that the bulk magnetisation and the magneto-crystalline anisotropy are non-collinear, the averaged magnetisation of the interface is expected to differ in such a case from the bulk one, thus explicitly breaking spin rotation invariance around the bulk mag-

netisation axis. (D) Finally, for mesoscopic interfaces there is a possibility for sample specific mesoscopic fluctuations in the spin configuration.

### Scattering matrix

It is known that any scattering matrix has a singular value decomposition

$$\hat{\mathbf{S}} = \begin{pmatrix} U & 0 \\ 0 & \tilde{U} \end{pmatrix} \begin{pmatrix} R & T \\ T^\dagger & -\underline{R} \end{pmatrix} \begin{pmatrix} V & 0 \\ 0 & \tilde{V} \end{pmatrix} \quad (\text{S8})$$

where  $U$  and  $V$  are unitary  $m \times m$  matrices,  $\tilde{U}$  and  $\tilde{V}$  are unitary  $n \times n$  matrices, the matrix  $T$  has only non-zero elements on the diagonal, that describe the transmission eigenvalues (real,  $0 < t < 1$ ) between the  $m$  channels on one side of the interface and the  $n$  channels on the other side (the number of transmission channels is the smaller of the two numbers  $m$  and  $n$ ).  $R = \sqrt{1 - TT^\dagger}$  and  $\underline{R} = \sqrt{1 - T^\dagger T}$  are diagonal matrices with the reflection eigenvalues. In our case, the scattering matrix (for each fixed momentum component parallel to the interface) connects two spin channels in the superconductor with one spin channel in the half metal. Consequently, in our case  $m = 2$  and  $n = 1$ , and  $\hat{\mathbf{S}}$  is a 3x3 matrix in spin space with

$$R = \begin{pmatrix} \sqrt{1-t^2} & 0 \\ 0 & 1 \end{pmatrix}, \quad \underline{R} = \sqrt{1-t^2}, \quad T = \begin{pmatrix} t \\ 0 \end{pmatrix}. \quad (\text{S9})$$

The 2x2 matrices  $U$  and  $V$  can be written in the form  $U = e^{i(\psi_u + \frac{\vartheta}{2} \mathbf{m} \cdot \boldsymbol{\sigma})}$ ,  $V = e^{i(\psi_v + \frac{\vartheta}{2} \mathbf{m} \cdot \boldsymbol{\sigma})}$ , and the scalars  $\tilde{U}$  and  $\tilde{V}$  are just phase factors  $\tilde{U} = e^{i\psi_{\tilde{u}}}$ ,  $\tilde{V} = e^{i\psi_{\tilde{v}}}$ . The scalar phases  $\psi_{u,v}$  and  $\psi_{\tilde{u},\tilde{v}}$  are irrelevant for the Josephson current, as they drop out of the final expressions; thus, for convenience we put them to zero.

The unit vector  $\mathbf{m}$  characterises the direction of the interface magnetisation (averaged over an area comparable with the size of a Cooper pair); the direction of the magnetisation  $\mathbf{M}$  of the half metal is the  $z$ -direction. In a system with spin rotation invariance around  $\mathbf{M}$  the directions  $\mathbf{m}$  and  $\mathbf{M}$  coincide. This is, however, not the case if spin rotation symmetry around  $\mathbf{M}$  is broken. We denote the angle between  $\mathbf{m}$  and  $\mathbf{M}$  by  $\alpha$ . Without loss of generality the spin quantisation axis in the superconductor can be chosen as the  $\mathbf{m}$ -axis, and in the half metal as the  $z$ -axis. The corresponding spin rotation matrix is  $U_m = e^{-i\frac{\alpha}{2} \mathbf{e}_\perp \cdot \boldsymbol{\sigma}}$  with  $\mathbf{e}_\perp = (\mathbf{m} \times \mathbf{M}) / (M \sin \alpha)$ . In this representation  $U_m U U_m^\dagger = e^{i\frac{\vartheta}{2} \sigma_z}$  and  $U_m V U_m^\dagger = e^{i\frac{\vartheta}{2} \sigma_z}$  become spin-diagonal, however the transmission vector  $T$  acquires a non-zero spin-flip component,  $U_m T = (t \cos \frac{\alpha}{2}, -t \sin \frac{\alpha}{2} e^{i\varphi})^{tr}$  where  $\varphi$  is the angle of  $\mathbf{m}$  in the

plane perpendicular to  $\mathbf{M}$ . This leads to

$$\hat{\mathbf{S}} = \left( \begin{array}{cc|c} r_{\uparrow\uparrow} e^{i\frac{\vartheta}{2}} & r_{\uparrow\downarrow} e^{i(\vartheta_{\uparrow\uparrow} - \vartheta_{\downarrow\uparrow})} & t_{\uparrow\uparrow} e^{i(\vartheta_{\uparrow\uparrow} + \frac{\vartheta}{4})} \\ r_{\downarrow\downarrow} e^{-i(\vartheta_{\uparrow\uparrow} - \vartheta_{\downarrow\uparrow})} & r_{\downarrow\downarrow} e^{-i\frac{\vartheta}{2}} & t_{\downarrow\downarrow} e^{i(\vartheta_{\downarrow\downarrow} - \frac{\vartheta}{4})} \\ \hline t_{\uparrow\uparrow} e^{-i(\vartheta_{\uparrow\uparrow} - \frac{\vartheta}{4})} & t_{\downarrow\downarrow} e^{-i(\vartheta_{\downarrow\downarrow} + \frac{\vartheta}{4})} & -r \end{array} \right), \quad (\text{S10})$$

with  $t_{\uparrow\uparrow} = t \cos \frac{\alpha}{2}$ ,  $t_{\downarrow\downarrow} = t \sin \frac{\alpha}{2}$ ,  $r_{\uparrow\uparrow} = \sin^2 \frac{\alpha}{2} + r \cos^2 \frac{\alpha}{2}$ ,  $r_{\downarrow\downarrow} = \cos^2 \frac{\alpha}{2} + r \sin^2 \frac{\alpha}{2}$ ,  $r_{\uparrow\downarrow} = r_{\downarrow\uparrow} = -\frac{1-r}{2} \sin \alpha$ ,  $r = \sqrt{1-t^2}$ ,  $\vartheta = \vartheta_u + \vartheta_v$ ,  $\vartheta_{\uparrow\uparrow} = \frac{\vartheta_u - \vartheta_v}{4}$ , and  $\vartheta_{\downarrow\downarrow} = \pi + \varphi + \vartheta_{\uparrow\uparrow}$ , which reduces for  $t \ll 1$  to the scattering matrix given in equation (1) of the paper.

## Methods

We obtain the Josephson current as function of impurity concentration, temperature and junction length using the quasiclassical Green's functions technique [4, 5]. The Green's functions  $\hat{g}(\mathbf{p}_F, \mathbf{R}, \varepsilon_n)$  depend on the spatial coordinate  $\mathbf{R}$ , Matsubara energy  $\varepsilon_n = (2n+1)\pi T$ , and the momentum direction on the Fermi surface  $\mathbf{p}_F$ . In the superconductors, the propagator  $\hat{g}$  is a 4x4 matrix in combined spin and particle-hole space,

$$\hat{g}^S = \left( \begin{array}{cc} g_s + \mathbf{g}_t \cdot \boldsymbol{\sigma} & (f_s + \mathbf{f}_t \cdot \boldsymbol{\sigma}) i\sigma_y \\ (\tilde{f}_s + \tilde{\mathbf{f}}_t \cdot \boldsymbol{\sigma}^*) i\sigma_y & \tilde{g}_s + \tilde{\mathbf{g}}_t \cdot \boldsymbol{\sigma}^* \end{array} \right), \quad (\text{S11})$$

where  $f_s$  and  $\mathbf{f}_t$  are singlet and triplet pairing amplitudes,  $g_s$  and  $\mathbf{g}_t$  are spin scalar and spin vector parts of the diagonal Green function, and the vector  $\boldsymbol{\sigma} = (\sigma_x, \sigma_y, \sigma_z)$  is composed of Pauli spin matrices. The hole amplitudes are related to the particle amplitudes by the symmetry  $\tilde{f}(\mathbf{p}_F, \varepsilon_n) = f(-\mathbf{p}_F, \varepsilon_n)^*$ . In the half metal, only conduction electrons with spin up exist, and the propagator is a 2x2 matrix in particle-hole space,

$$\hat{g}^H = \left( \begin{array}{cc} g_{\uparrow\uparrow} & f_{\uparrow\uparrow} \\ \tilde{f}_{\uparrow\uparrow} & \tilde{g}_{\uparrow\uparrow} \end{array} \right). \quad (\text{S12})$$

The propagators are connected at the interfaces via the scattering matrices given in equation (1) of the paper.

The transport equation governing the supercurrent in the heterostructure is given by the Eilenberger equation for the propagator  $\hat{g}$ . Impurities are treated in the Born approximation using a life time  $\tau_S$  of quasiparticles in the superconductor, and a life time  $\tau_H$  in the half metal. The corresponding mean free paths are  $\ell_S = v_S \tau_S$ ,  $\ell_H = v_H \tau_H$ , with the Fermi velocities  $v_S$  and  $v_H$  in the two materials. The equation of motion for the 4x4 Green's function in the superconductors reads,

$$i v_S \mu \partial_x \hat{g} + \left[ i \varepsilon_n \hat{\tau}_3 - \hat{\Delta} - \frac{1}{2\pi\tau_S} \langle \hat{g} \rangle, \hat{g} \right] = \hat{0}, \quad (\text{S13})$$

where  $\mu = \cos(\theta_p)$ ,  $\theta_p$  is the angle between the Fermi velocity and the  $x$ -axis,  $\hat{\tau}_3$  is the third Pauli matrix in

symmetry	even frequency	odd frequency
even parity	$f_s^s = \frac{\pi \Delta \Omega_n (1 - \sin^2 \frac{\vartheta}{2})}{\Omega_n^2 -  \Delta ^2 \sin^2 \frac{\vartheta}{2}}$	$f_t^s = \frac{i \pi \Delta \varepsilon_n \frac{1}{2} \sin \vartheta}{\Omega_n^2 -  \Delta ^2 \sin^2 \frac{\vartheta}{2}}$
odd parity	$f_{t_0}^a = \frac{-i \pi \Delta \Omega_n s_\mu \frac{1}{2} \sin \vartheta}{\Omega_n^2 -  \Delta ^2 \sin^2 \frac{\vartheta}{2}}$	$f_s^a = \frac{\pi \Delta \varepsilon_n s_\mu \sin^2 \frac{\vartheta}{2}}{\Omega_n^2 -  \Delta ^2 \sin^2 \frac{\vartheta}{2}}$

TABLE S2: (Supplementary Table) Symmetry components of the interface amplitudes in the superconductors for the the clean limit, assuming a constant singlet order parameter  $\Delta$  and small tunnelling amplitudes ( $t \ll 1$ ). Here,  $\Omega_n = \sqrt{|\Delta|^2 + \varepsilon_n^2}$  and  $s_\mu = \text{sgn}(\mu)$ .

particle-hole space, and  $\hat{\Delta} = \Delta \hat{i} \sigma_y$  is the singlet order parameter. The average  $\langle \dots \rangle = \int \frac{d \cos(\theta_p) d\varphi_p}{4\pi} \dots$  is over all momentum directions. There is an analogous equation for the 2x2 Green's function in the half metal,

$$i v_H \mu \partial_x \hat{g} + \left[ i \varepsilon_n \hat{\tau}_3 - \frac{1}{2\pi\tau_H} \langle \hat{g} \rangle, \hat{g} \right] = \hat{0}. \quad (\text{S14})$$

Equations (S13)-(S14) are supplemented with the normalisation condition  $\hat{g}^2 = -\pi^2 \hat{1}$ .

We linearise the above equations for small triplet components in the superconductor ( $f_{t_0}$ ) and in the half metal ( $f_{\uparrow\uparrow}$ ). From the clean limit solutions for the interface amplitudes in the superconductors for  $t \ll 1$  and for a constant singlet order parameter  $\Delta$  (shown in Supplementary Table S2), we see that it is necessary, in order to ensure small  $f_{t_0}$ , to neglect higher order terms in the parameter  $\sin(\vartheta) \approx \vartheta$ . We will do so in the following. The correction to  $f_s^s$  are then of order  $\sin^2 \frac{\vartheta}{2}$ , leaving the order parameter unaffected in leading order in  $\vartheta$ . The normalisation condition is used to eliminate the diagonal part of  $\hat{g}$  in favour of a coupled set of equations for  $f$ -functions with positive and negative momentum directions. We decouple the system of differential equations by introducing the new triplet functions  $\Psi_{0j}$  and  $\Psi_j$  in equations (2)-(3) in the paper.

The solutions for the functions  $\Psi_{0j}^{s,a}$ , appearing in the ansatz Eq. (2) for the superconductors, are given by

$$\Psi_{01}^s(x) = \frac{s_\varepsilon}{2} B_{01}(x) + \int_{-\infty}^{x_1} dx' \frac{K_1(x, x')}{2|\mu|\ell_S} \langle \Psi_{01}^s(x') \rangle \quad (\text{S15})$$

$$\Psi_{02}^s(x) = \frac{s_\varepsilon}{2} B_{02}(x) + \int_{x_2}^{\infty} dx' \frac{K_2(x, x')}{2|\mu|\ell_S} \langle \Psi_{02}^s(x') \rangle \quad (\text{S16})$$

with  $s_\varepsilon = \text{sgn}(\varepsilon_n)$ ,  $B_{0j}(x) = e^{-|x-x_j|/\xi_S|\mu|}$ ,  $K_j(x, x') = e^{-|x-x'|/\xi_S|\mu|} + e^{-(|x'-x_j|+|x-x_j|)/\xi_S|\mu|}$ , and  $\xi_S = v_S/(2\Omega_n + \tau_S^{-1})$  with  $\Omega_n = \sqrt{\varepsilon_n^2 + |\Delta|^2}$ . The momentum-antisymmetric parts are obtained by using the identity  $\Psi_{0j}^a = -\mu s_\varepsilon \xi_S \partial_x \Psi_{0j}^s$ .

After using the boundary conditions with the scattering matrix  $\hat{\mathbf{S}}$  for  $\hat{g}^S$  and  $\hat{g}^H$ , we obtain the solutions  $\Psi_j^{s,a}$



in the half metal,

$$\Psi_j^s(x) = \frac{1}{1 - e^{-2L/\xi_H|\mu|}} \left( \frac{s_\varepsilon}{2} B_j(x) + \int_{x_1}^{x_2} dx' \frac{K(x, x')}{2|\mu|\ell_H} \langle \Psi_j^s(x') \rangle \right) \quad (\text{S17})$$

with  $\xi_H = v_H/(2|\varepsilon_n| + \tau_H^{-1})$ ,  $L = x_2 - x_1$ ,  $s_\varepsilon B_1(x) = \Psi_{01}^s(x_1) (e^{-(x-x_1)/\xi_H|\mu|} + e^{-(L+x_2-x)/\xi_H|\mu|})$ ,  $s_\varepsilon B_2(x) = \Psi_{02}^s(x_2) (e^{-(x_2-x)/\xi_H|\mu|} + e^{-(L+x-x_1)/\xi_H|\mu|})$ ,  $K(x, x') = e^{-|x-x'|/\xi_H|\mu|} + e^{-(2L-|x-x'|)/\xi_H|\mu|} + e^{-(x+x'-2x_1)/\xi_H|\mu|} + e^{-(2x_2-x-x')/\xi_H|\mu|}$ . The momentum-antisymmetric parts are obtained by using the identity  $\Psi_j^a = -\mu s_\varepsilon \xi_H \partial_x \Psi_j^s$ .

The integral equations (S15)-(S17) for  $\langle \Psi^s(x) \rangle$  are solved by replacing  $\Psi$  on a spatial grid with a piecewise linear function. Exact integration of the resulting expressions reduces the problem to a simple matrix inversion. The angular averages can be performed analytically and lead to exponential integrals. This procedure is necessary because the integration kernel decays on a different length scale compared with  $\Psi$  in the diffusive limit.

The current density in the half metal is given by the diagonal Green's function,

$$J_x(x) = ev_H N_H T \sum_{\varepsilon_n} \langle \mu g_{\uparrow\uparrow}(\mu, \varepsilon_n, x) \rangle, \quad (\text{S18})$$

where  $N_H$  is the density of states at the Fermi level for the conducting spin band in the half metal, and  $e$  is the electronic charge. It can be shown from the transport equations (S13) and (S14) that the current density  $J_x$  does in fact not depend on the spatial coordinate, in agreement with the continuity equation that expresses particle conservation.

Using the normalisation condition in the half metal,  $g_{\uparrow\uparrow}^2 = -\pi^2 - f_{\uparrow\uparrow} \tilde{f}_{\uparrow\uparrow}$ , for small triplet amplitudes, one obtains in leading order  $g_{\uparrow\uparrow} = -i\pi \text{sgn}(\varepsilon_n) (1 + f_{\uparrow\uparrow} \tilde{f}_{\uparrow\uparrow} / 2\pi^2)$ , leading to

$$J_x = \frac{ev_H N_H T}{2\pi i} \sum_{\varepsilon_n} \langle \mu f_{\uparrow\uparrow}(\mu, \varepsilon_n, x) \tilde{f}_{\uparrow\uparrow}(\mu, \varepsilon_n, x) \rangle \text{sgn}(\varepsilon_n). \quad (\text{S19})$$

It is instructive to decompose the anomalous propagators into their symmetric and antisymmetric part  $f_{\uparrow\uparrow}^{s,a}$  with respect to  $\mu$ . Doing this and using the fundamental symmetries  $f_{\uparrow\uparrow}^s(-\varepsilon_n) = -f_{\uparrow\uparrow}^s(\varepsilon_n)$ ,  $f_{\uparrow\uparrow}^a(-\varepsilon_n) = f_{\uparrow\uparrow}^a(\varepsilon_n)$  we arrive at

$$J_x = -\frac{2ev_H N_H T}{\pi} \sum_{\varepsilon_n > 0} \int_0^1 d\mu \mu \text{Im}(f_{\uparrow\uparrow}^s f_{\uparrow\uparrow}^{a*}). \quad (\text{S20})$$

Substitution of equation (3) of the paper into equation (S20) leads to equations (6)-(7) of the paper.

To study the symmetry properties of the Josephson current, we expand the pairing amplitudes in Legendre polynomials. Writing  $\bar{\Psi}_j(\mu) = A_j(\mu) \Psi_j(\mu)$ , the expansion is  $\bar{\Psi}_j(\mu) = \sum_{l=0}^{\infty} P_l(\mu) \bar{\Psi}_{j,l}$ , with components

Superconductor side: $\ell_S = v_S \tau_S$	
	$\xi_S = \frac{v_S}{2\Omega_n + \tau_S^{-1}}$
	$\tilde{\xi}_0 = \frac{v_S}{2\pi T_c}$
Half-metallic side: $\ell_H = v_H \tau_H$	
	$\xi_H = \frac{v_H}{2 \varepsilon_n  + \tau_H^{-1}}$
	$\xi_c = \frac{v_H}{2\pi T}$
	$\xi_0 = \frac{v_H}{2\pi T_c}$
	$\xi_d = \sqrt{\frac{\ell_H \xi_c}{3}} = \sqrt{\frac{D}{2\pi T}}$
	$\xi_D = \sqrt{\frac{\ell_H \xi_0}{3}} = \sqrt{\frac{D}{2\pi T_c}}$

TABLE S3: (Supplementary Table) Collection of various length scales that enter in the problem. Here  $v_S$  and  $v_H$  are Fermi velocities in the superconductor and the half-metal, respectively, while  $\tau_S$  and  $\tau_H$  are the impurity scattering times in the two materials, and  $D$  is the diffusion constant in the half metal.

$\bar{\Psi}_{j,l} = (2l+1) \langle P_l(\mu) \bar{\Psi}(\mu) \rangle$ . Using that

$$\int_0^1 d\mu \mu (\bar{\Psi}_2^s \bar{\Psi}_1^a - \bar{\Psi}_1^s \bar{\Psi}_2^a) = \sum_{l=0}^{\infty} \frac{(-1)^l (l+1)}{(2l+1)(2l+3)} (\bar{\Psi}_{2,l} \bar{\Psi}_{1,l+1} - \bar{\Psi}_{1,l} \bar{\Psi}_{2,l+1}), \quad (\text{S21})$$

we can bring equation (7) in the paper to the form  $J_c = \sum_{l=0}^{\infty} J_{c;l,l+1}$ .

The various length scales appearing in the paper are listed in Supplementary Table S3.

## Supplementary Results

In Supplementary Fig. S1 we show solutions of the integral equations in the superconductor, equations (S15)-(S16), and in the half metal, equation (S17), for several impurity concentrations ranging from the ballistic limit to the diffusive limit. The triplet amplitudes in the superconductor are  $m = 0$  with respect to the interface moments, and in the half metal are equal-spin  $m = 1$  amplitudes with respect to the bulk magnetisation axis  $\mathbf{M}$ . The interface moments can be misaligned with respect to  $\mathbf{M}$  as result of a (spontaneous or induced) breaking of spin-rotation symmetry around  $\mathbf{M}$  at the interface. The symmetry components in the half metal are defined as

$$F_j^s(x) = T \sum_{\varepsilon_n > 0} \langle f_{\uparrow\uparrow j}(x) \rangle \frac{|\Delta|}{\Omega_n}, \quad (\text{S22})$$

$$F_j^p(x) = \frac{1}{3} T \sum_{\varepsilon_n > 0} \langle \mu f_{\uparrow\uparrow j}(x) \rangle \frac{|\Delta|}{\Omega_n}. \quad (\text{S23})$$

In the superconductor an analogous definition holds for the  $m = 0$  components  $F_{t_0 j}^s$  and  $F_{t_0 j}^p$ . In the left panels

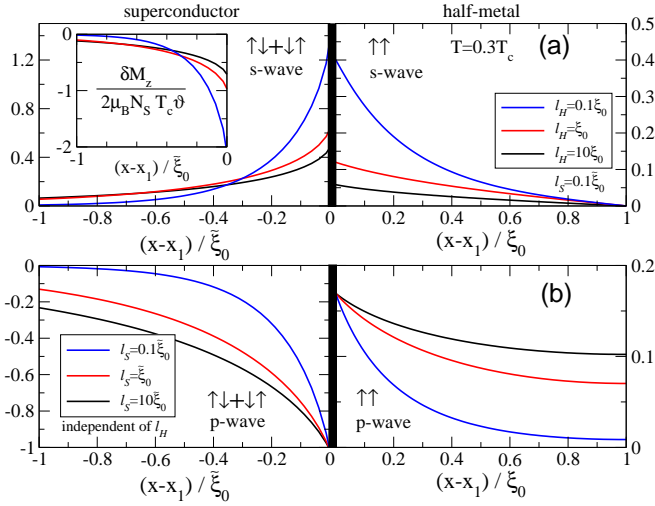


FIG. S1: (Supplementary Figure) Spatial dependences of pairing amplitudes in the superconductor (in units of  $\sin(\vartheta)|\Delta|e^{i\chi_j}$ ) and in the half metal (in units of  $iA_j|\Delta|e^{i\chi_j}$ , length  $L = 2\xi_0$ , only left half shown) for a  $\pi$ -junction. The odd-frequency  $s$ -wave triplet amplitude is shown in the upper panel, the even-frequency  $p$ -wave triplet amplitude in the lower panel. In the inset we show the induced spin polarisation of quasiparticles near the interface in the superconductor.

of Supplementary Fig. S1 we vary the superconducting mean free path  $\ell_S$ , and in the right panels the half metal mean free path  $\ell_H$  for fixed  $\ell_S$ . Whereas the interface value of  $F_{t_0j}^p$  in the superconductor does not change with varying mean free path, the interface value of  $F_{t_0j}^s$  increases with decreasing mean free path in the superconductor,  $\ell_S$ , as  $1/\sqrt{\ell_S}$  until it reaches values comparable with the singlet amplitude. Their decay length in the superconductors decreases, and changes from  $(\xi_S^{-1} + \ell_S^{-1})^{-1}$  in the ballistic limit to  $\sqrt{\xi_S \ell_S / 3}$  in the diffusive limit. An analogous picture is seen on the half-metallic side.

In the inset we also show the induced spin polarisation in the superconductors. It is calculated from the diagonal part of the Green's function, given (for small  $\vartheta_j$ ) by

$$g_{zj}(x) = -\pi \frac{|\Delta|^2 \sin \vartheta_j}{\varepsilon_n^2 + |\Delta|^2} \text{sgn}(\varepsilon_n) \Psi_{0j}^s(x). \quad (\text{S24})$$

There is, consequently, a surface spin polarisation in the superconductor, that in the clean limit is given by

$$\langle g_{zj}(x) \rangle = -\frac{\pi |\Delta|^2}{2(\varepsilon_n^2 + |\Delta|^2)} \langle \sin \vartheta_j e^{-|x-x_j|/\xi_S |\mu|} \rangle. \quad (\text{S25})$$

The induced spin magnetisation is then

$$\delta M_z(x) = 2\mu_B N_S T \sum_{\varepsilon_n} \langle g_{zj}(x) \rangle, \quad (\text{S26})$$

where  $\mu_B$  is the Bohr magneton and  $N_S$  is the density of states in the superconductor.

In Supplementary Fig. S2 we present an analysis of the spatial dependences of the odd-frequency  $s$ -wave and

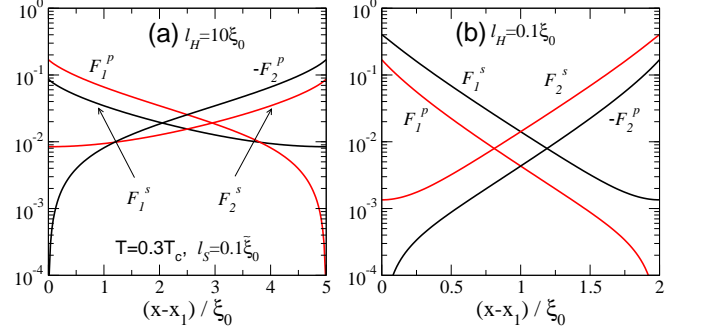


FIG. S2: (Supplementary Figure) Role of triplet correlation functions in the half metal. The contribution to the Josephson current from the  $s$ -wave  $\uparrow\uparrow$ -triplet correlation function always enters as a product with the  $p$ -wave  $\uparrow\uparrow$ -triplet, with one of the two originating from the left superconductor and the other from the right. For clean half metals, shown in (a), the  $p$ -wave component is larger than the  $s$ -wave. For more dirty structures, shown in (b), the  $p$ -wave component is suppressed compared with the  $s$ -wave and the Josephson current is suppressed accordingly. Amplitudes are plotted in units of  $iA_j|\Delta|e^{i\chi_j}$ .

even-frequency  $p$ -wave pairing amplitudes in the half metal. We show for the ballistic case ( $\ell_H = 10\xi_0$ ) and for the diffusive case ( $\ell_H = \xi_0/10$ ) the pairing amplitudes induced from the left and right interfaces. By multiplying the two black curves with each other and the two red curves with each other, and summing the two contributions, we obtain a quantity related to the  $s$ - $p$  contribution to the Josephson current [see equation (7)]. For ballistic systems the  $p$ -wave amplitudes are larger than the  $s$ -wave amplitudes near the interfaces, while the opposite holds for diffusive systems. Amplitudes for fixed frequency give a similar picture.

- 
- [1] Keizer, R.S. *et al.* A spin triplet supercurrent through the half-metallic ferromagnet CrO<sub>2</sub>. *Nature* **439**, 825-827 (2006).
  - [2] S.T.B. Goennenwein *et al.*, *Appl. Phys. Lett.* **90**, 142509 (2007).
  - [3] Reddy B.V., Khanna, S.N. & Ashman, C. Oscillatory magnetic coupling in Cr<sub>2</sub>O<sub>n</sub> ( $n = 1 - 6$ ) clusters. *Phys. Rev. B* **61**, 5797-5801 (2000).
  - [4] Eilenberger, G. Transformation of Gorkov's Equation for Type II Superconductors into Transport-Like Equations. *Z. Phys.* **214**, 195-213 (1968).
  - [5] Larkin, A. I. & Ovchinnikov, Y. N. Quasiclassical Method in Theory of Superconductivity. *Zh. Eksp. Teor. Fiz.* **55**, 2262-& (1968), [*Sov. Phys. JETP* **28**, 1200-& (1969)].